International Electronic Journal of Geometry
Volume 5 No. 1 pp. 1–35 (2012) ©IEJG

THE MINKOWSKIAN PLANAR 4R MECHANISM

GÁBOR HEGEDÜS AND BRIAN MOORE

(Communicated by Yusuf YAYLI)

Abstract. We characterize and classify completely the planar 4R closed chain working on the Minkowskian plane. Our work would open a new research direction in the theory of geometric designs: the classification and characterization of the geometric design of linkages working in non–Euclidean spaces.

1. Introduction

First we recall here some preliminary definitions and results from the geometry of linkages.

A linkage is a collection of interconnected components, individually called *links*. The *joint* is the physical connection between two links.

In our article we consider only the *revolute* joint, which can be viewed as constructed from the rotary hinge. We denote the revolute joint by R.

The revolute joint allows *one-degree-of-freedom* movement between the two links that it connects. The configuration variable for a hinge is the angle measured around its axis between the two bodies.

Of course we can form linkages from other joints, for example the universal joint, the ball-in-socket and the *prismatic* joint.

The *generic mobility* of the system is the number of independent parameters such as the joint angles that are needed to specify the configuration of the linkage.

On the other hand it can be shown that this is the dimension of the *configuration space* of the system.

A *planar* linkage has the property that all of its links move in parallel planes. We are interested here in the four–bar linkage, which is a closed chain formed by four links and four joints. Figure 1 is an example of a planar 4R closed chain.

The usual model of geometric designs are working in the Euclidean space. In this article we would like to characterize and classify completely the planar 4R closed chain working on the Minkowskian plane. This work would open a new research

Date: Received: February 07, 2011 and Accepted: January 15, 2012.
2010 *Mathematics Subject Classification.* 51P05, 53A17, 70B15.
Key words and phrases. Mechanism, Minkowskian space, double numbers.

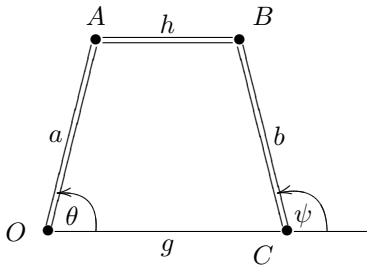

FIGURE 1. The planar 4R linkage

direction in the theory of geometric designs: the classification and characterization of the geometric design of linkages working in non–Euclidean spaces.

A. Einstein published in 1905 his famous paper [5] which later became known as his introduction to the special relativity theory. In 1907 Minkowski gave a geometrical interpretation of the special relativity space–time using 4–dimensional Minkowskian spaces and Lorentz transformations.

Later P. Fjelstad used the perplex number system to exploit this connection with special relativity (see [6]).

This mathematical tool based on the hyperbolic numbers, introduced by S. Lie in the late XIX century (see [9]).

One of our main motivation to consider the Minkowskian planar 4R mechanism was to connect the geometric theory of special relativity to the geometric design of linkages. We do not see obvious interpretation of our work in theoretical physics, but we hope we can motivate later such research.

In Chapter 2 we collected the preliminary definitions and results about the Minkowskian plane and hyperbolic trigonometry. In Chapter 3 we describe our main results: the position analysis and the classification of the Minkowskian 4R planar linkage. We give also an exact formula for the coupler curve of this system and compute the transmission and coupler angles.

2. PRELIMINARIES

2.1. **The Minkowskian plane and the double numbers.** First we give an algebraic description of the Minkowskian plane.

In analogy with the complex number system, the system of *double numbers* [1] can be introduced:

$$\mathbb{H} := \{x + jy : \ x, y \in \mathbb{R}, \ j^2 = 1\}$$

Here j is the *double imaginary unit* and x and y are respectively called the *real* and the *unipotent* parts of the double number $z = x + yj$.

It follows that multiplication in $\mathbb{H}$ is defined by $(x + yj)(r + sj) = (xr + ys) + j(xs + yr)$.

[1] these numbers are called to split–complex numbers, too

It is known that the complex numbers are related to the Euclidean geometry. Similarly the double system of numbers serve as coordinates in the Minkowskian plane (space-time geometry, see [6]).

The *hyperbolic conjugate* $\overline{z}$ of $z = x + yj$ is defined by $\overline{z} = x - yj$.

The *hyperbolic scalar product* is given by

$$\langle z, w\rangle := Re(z\overline{w}) = xu - yv,$$

where $z = x + yj$ and $w = u + jv$. We say that the double numbers z and w are *double–orthogonal*, if $\langle z, w\rangle = 0$.

We define the *hyperbolic modulus* of $z = x + yj$ by

$$\| z\|_h := \sqrt{|\langle z, z\rangle|} = \sqrt{|z\overline{z}|} = \sqrt{|x^2 - y^2|} \geq 0. \tag{2.1}$$

We can consider this modulus as the *hyperbolic distance* of the point z from the origin.

It can be shown that this modulus is the Lorentz invariant of two dimensional special relativity, see [16].

Note that the points $z \neq 0$ on the lines $y = x$ and $y = -x$ are isotropic. This means that they are nonzero vectors with $\| z \|_h = 0$.

For $r \in \mathbb{R}^+$ the *Minkowskian circle* of radius r centered at the origin in $\mathbb{H}$ is defined by

$$\{(x, y) \in \mathbb{R} : \ x^2 - y^2 = r^2\}$$

Clearly this set is the set of all points in the Minkowskian plane that satisfy the equation $\| z \|_h^2 = r^2$ (see Figure 2).

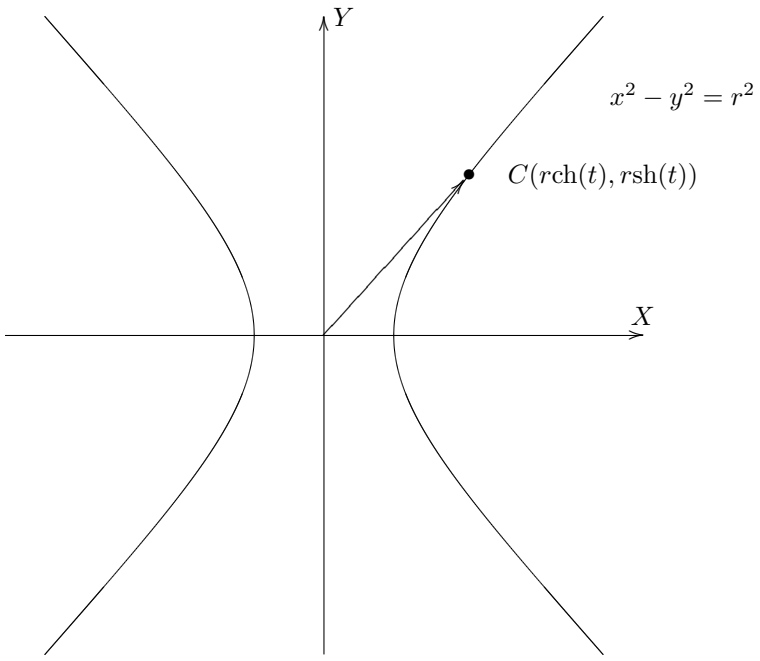

FIGURE 2. The Minkowskian circle of radius r centered at the origin

We can remind here for the following analog of Euler's formula for the double numbers $z = x + yj$:

$$z = re^{j\phi} = r(\mathrm{ch}\,(\phi) + j\mathrm{sh}\,(\phi))$$

where $x^2 - y^2 > 0$ and $y > 0$.

2.2. **Hyperbolic trigonometry.** Let $L := L^2$ denote the vector space $\mathbb{R}^2$ provided with the hyperbolic scalar product.

We denote by $SO^+(1,1)$ the *proper Lorentzian group* consisting of all matrices of the form

$$A(\phi) = \begin{pmatrix} \mathrm{ch}\,(\phi) & \mathrm{sh}\,(\phi) \\ \mathrm{sh}\,(\phi) & \mathrm{ch}\,(\phi) \end{pmatrix},$$

where $\phi \in \mathbb{R}$, see [1], [16].

In L^2 a Lorentzian vector $\underline{u}$ is called to *spacelike*, *lightlike* or *timelike* if $\langle \underline{u}, \underline{u} \rangle_L > 0$, $\langle \underline{u}, \underline{u} \rangle_L = 0$ or $\langle \underline{u}, \underline{u} \rangle_L < 0$, respectively.

We say that a timelike vector $\underline{u} = (u_1, u_2)$ is *left–pointing* or *right–pointing* if $u_2 > 0$ or $u_2 < 0$, respectively. Similarly, a spacelike vector $\underline{u} = (u_1, u_2)$ is *left–pointing* or *right–pointing* if $u_1 > 0$ or $u_1 < 0$, respectively (see [12]). The following Lemma was proven in [1].

Lemma 2.1. *(Reversed triangle inequality) Let $\underline{x}$ and $\underline{y}$ be left–pointing timelike vectors in L^2. Then $\underline{x} + \underline{y}$ is a left–pointing timelike vector and*

$$\| \underline{x} + \underline{y} \| \geq \| \underline{x} \| + \| \underline{y} \| .$$

Here the equality holds iff $\underline{y} = c\underline{x}$ for some $c > 0$.

Lemma 2.2. *Let $\underline{x}$ and $\underline{y}$ be left–pointing spacelike vectors in L^2. Then $\underline{x} + \underline{y}$ is a left–pointing spacelike vector and*

$$\| \underline{x} + \underline{y} \| \geq \| \underline{x} \| + \| \underline{y} \| .$$

Here the equality holds iff $\underline{y} = c\underline{x}$ for some $c > 0$.

Proof. Suppose that $\underline{x} = \overrightarrow{AB}$, $\underline{y} = \overrightarrow{BC}$ and $\underline{x} + \underline{y} = \overrightarrow{AC}$. Now after reflecting the points A, B and C to the line $\underline{y} = \underline{x}$ we get the points A', B' and C'. Let $\underline{d} := \overrightarrow{A'B'}$ and $\underline{e} := \overrightarrow{B'C'}$. Then $\underline{d} + \underline{e} = \overrightarrow{A'C'}$ and it comes from the definition of the norm that

$$\| \underline{x} \| = \| \underline{d} \|, \ \| \underline{y} \| = \| \underline{e} \| \ \text{ and } \ \| \underline{d} + \underline{e} \| = \| \underline{x} + \underline{y} \| .$$

Hence using Lemma 2.1 we get that

$$\| \underline{d} + \underline{e} \| = \| \underline{x} + \underline{y} \| \geq \| \underline{x} \| + \| \underline{y} \| = \| \underline{d} \| + \| \underline{e} \| .$$

□

Corollary 2.1. *Suppose that $OABC$ is a quadrilateral where $a = \| \overrightarrow{OA} \|$, $b = \| \overrightarrow{BC} \|$, $g = \| \overrightarrow{OC} \|$, $h = \| \overrightarrow{AB} \|$. Suppose that $\overrightarrow{OA}$, $\overrightarrow{BC}$, $\overrightarrow{OC}$ and $\overrightarrow{AB}$ are left–pointing spacelike vectors (see Figure 1). Then $g \geq a + b + h$.*

Moreover, if $g = a + b + h$, then the vectors $\overrightarrow{OA}$, $\overrightarrow{BC}$, $\overrightarrow{OC}$ and $\overrightarrow{AB}$ are collinear.

Proof. The inequality $g \geq a + b + h$ is a direct consequence of Lemma 2.2.

Now, assume that $g = a + b + h$. We prove first that the vectors $\overrightarrow{OC}$ and $\overrightarrow{OB}$ are collinear. Suppose, indirectly, that $\overrightarrow{OC}$ and $\overrightarrow{OB}$ are not collinear. Since $\overrightarrow{OB}$ is a

left–pointing spacelike vector, hence we can apply the reversed triangle inequality (Lemma 2.2) for the triangle OBC. Then it follows that

$$g = \| \overrightarrow{OC} \| > \| \overrightarrow{OB} \| + \| \overrightarrow{BC} \| = b + \| \overrightarrow{OB} \|$$

We can apply again Lemma 2.2 for the triangle OAB. Hence

$$\| \overrightarrow{OB} \| \geq a + h.$$

Consequently

$$g = \| \overrightarrow{OC} \| > a + b + h,$$

which is a contradiction.

Similar argument shows that $\overrightarrow{OB}$ and $\overrightarrow{OA}$ are colllinear. Hence $\overrightarrow{OC}$ and $\overrightarrow{OA}$ are collinear. We can use very similar arguments to prove that $\overrightarrow{OA}$ and $\overrightarrow{AB}$ are collinear vectors. So the result follows. □

We define now the notion of angle on the Minkowskian plane.

Let $\underline{x}$ and $\underline{y}$ be two left–pointing timelike unit vectors. We say that $\phi \in \mathbb{R}$ is the *(oriented) angle* from $\underline{x}$ to $\underline{y}$ if $A(\phi)\underline{x} = \underline{y}$. The (unoriented) angle between $\underline{x}$ and $\underline{y}$ is defined to be $|\phi|$. Then it comes from the definition that

$$\mathrm{ch}\,(\phi) = -\langle \underline{x}, \underline{y} \rangle_L,$$

where the right-hand side is greater than 1.

When $\underline{x}$ and $\underline{y}$ are left–pointing timelike vectors, than the angle ϕ for $\underline{x}$ and $\underline{y}$ is the same as for $\underline{x}/\| \underline{x} \|$ and $\underline{y}/\| \underline{y} \|$.

We have

$$\mathrm{ch}\,(\phi) = -\frac{\langle \underline{x}, \underline{y} \rangle_L}{\| \underline{x} \| \| \underline{y} \|}$$

We can give the same definition for the angle between left–pointing spacelike vectors. From this definition, we obtain similar formula for $\mathrm{ch}\,(\phi)$: if $\underline{x}$ and $\underline{y}$ are two left–pointing spacelike unit vectors, then

$$\mathrm{ch}\,(\phi) = \langle \underline{x}, \underline{y} \rangle_L,$$

where ϕ is the (oriented) angle from $\underline{x}$ to $\underline{y}$.

In the Euclidean plane, a motion can be represented by a combination of a rotation and translation. It is well–known that any motion can be expressed using the matrix operation

$$M(t,a,b) \begin{pmatrix} x_1 \\ x_2 \\ 1 \end{pmatrix} = \begin{pmatrix} \cos(t) & -\sin(t) & a \\ \sin(t) & \cos(t) & b \\ 0 & 0 & 1 \end{pmatrix} \begin{pmatrix} x_1 \\ x_2 \\ 1 \end{pmatrix}$$

Similarly, for the Minkowskian plane the group of motions is the following:

$$\overline{G} := \left\{ \begin{pmatrix} \mathrm{ch}\,(t) & \mathrm{sh}\,(t) & a \\ \mathrm{sh}\,(t) & \mathrm{ch}\,(t) & b \\ 0 & 0 & 1 \end{pmatrix} : \ t, a, b \in \mathbb{R} \right\}$$

We now introduce an important class of triangles. By a *pure triangle* we mean a triangle with vertices A, B and C such that $\overrightarrow{AB}$ and $\overrightarrow{BC}$ are left–pointing timelike vectors. In the following we assume that we named the vertices of a pure triangle ABC in this manner. The angle $\widehat{C}$ is the angle between the lines BC and AC.

Finally we recall here for the Minkowskian cosine rule:

Theorem 2.1. *(see* [1, Theorem 7]*) Let* $\triangle ABC$ *be a pure triangle. Then*

$$c^2 = a^2 + b^2 - 2ab\mathrm{ch}(\widehat{C}) \tag{2.2}$$

where $a = \| \overrightarrow{BC} \|$, $b = \| \overrightarrow{AC} \|$ *and* $c = \| \overrightarrow{AB} \|$.

□

Remark 2.1. It can be shown (see [14]) that Theorem 2.1 holds for any pure triangles such that all its sides $\overrightarrow{AB}$, $\overrightarrow{AC}$ and $\overrightarrow{BC}$ are spacelike vectors.

3. The main results

3.1. **Position Analysis of the Minkowskian 4R linkage.** Recall that the four-bar linkage is a mechanism that lies in the plane and consists of four bars connected by joints that allow rotation only in the plane of the mechanism, see Figure 1.

Throughout this Chapter we suppose that $\overrightarrow{OA}$, $\overrightarrow{OC}$ and $\overrightarrow{CB}$ are left–pointing spacelike vectors. Suppose that $\overrightarrow{AB}$ is a spacelike vector.

Let the fixed and the moving pivots of the input crank be O and A, respectively.

Let the fixed and the moving pivots of the output crank be C and B, respectively. We define the distances between these points as follows:

$$a := \| \overrightarrow{OA} \|,\ b := \| \overrightarrow{BC} \|,\ g := \| \overrightarrow{OC} \|,\ h := \| \overrightarrow{AB} \| .$$

To analyse the linkage, we locate the origin in the fixed Minkowskian frame F at O and orient it so that the x-axis passes through the other fixed pivot C.

Theorem 3.1. *Let* θ *be the input angle measured around* O *from the* x*-axis of* F *to* OA*. Let* ψ *be the angular position of the output crank* CB *(see Figure 1). Then*

$$\psi = 2artanh\frac{-B(\theta) \pm \sqrt{B(\theta)^2 + C(\theta)^2 - A(\theta)^2}}{A(\theta) + C(\theta)}, \tag{3.1}$$

where

$$A(\theta) = 2gb - 2abch(\theta),$$
$$B(\theta) = 2absh(\theta),$$

and

$$C(\theta) = h^2 - g^2 - b^2 - a^2 + 2agch(\theta).$$

Proof. Since $h = \| \overrightarrow{AB} \|$ is constant, we get the constraint equation as

$$\| \overrightarrow{AB} \|^2 = h^2. \tag{3.2}$$

It is easy to verify that the coordinates of A and B is given by $A = (a\mathrm{ch}(\theta), a\mathrm{sh}(\theta))$ and

$$B = (g + b\mathrm{ch}(\psi), b\mathrm{sh}(\psi)). \tag{3.3}$$

If we substitute these coordinates into (3.2), then we obtain

$$b^2 + g^2 + a^2 + 2gb\mathrm{ch}(\psi) - 2ag\mathrm{ch}(\theta) - 2ab\mathrm{ch}(\psi)\,\mathrm{ch}(\theta) + 2ab\mathrm{sh}(\psi)\,\mathrm{sh}(\theta) = h^2.$$

If we gather the coefficients of $\mathrm{ch}(\psi)$ and $\mathrm{sh}(\psi)$, we obtain the constraint equation for the 4R chain as

$$A(\theta)\mathrm{ch}(\psi) + B(\theta)\mathrm{sh}(\psi) = C(\theta), \tag{3.4}$$

where

$$A(\theta) = 2gb - 2ab\mathrm{ch}(\theta),$$

$$B(\theta) = 2ab\mathrm{sh}\,(\theta)\,,$$

and

$$C(\theta) = h^2 - g^2 - b^2 - a^2 + 2ag\mathrm{ch}\,(\theta)\,.$$

We solve this equation using the tan-half-technique. This technique uses a transformation of variables to convert $\mathrm{ch}\,(\psi)$ and $\mathrm{sh}\,(\psi)$ into algebraic functions of $\mathrm{th}\,(\psi/2)$.

Introduce the parameter $y = \mathrm{th}\,(\psi/2)$, which allows us to define

$$\mathrm{ch}\,(\psi) = \frac{1+y^2}{1-y^2} \text{ and } \mathrm{sh}\,(\psi) = \frac{2y}{1-y^2}$$

Substitute into (3.4) to obtain

$$(A(\theta) + C(\theta))y^2 + 2B(\theta)y + A(\theta) - C(\theta) = 0.$$

This equation is solved using the quadratic formula to obtain

$$\mathrm{th}\,(\psi/2) = \frac{-B(\theta) \pm \sqrt{B(\theta)^2 + C(\theta)^2 - A(\theta)^2}}{A(\theta) + C(\theta)}.$$

□

Remark 3.1. It can be derived the following alternative equation for ψ:

$$\psi = -\mathrm{artanh}\frac{B(\theta)}{A(\theta)} \pm \mathrm{arch}\frac{C(\theta)}{\sqrt{A(\theta)^2 - B(\theta)^2}}.$$

Namely we infer from (3.4) that

$$\frac{A(\theta)}{\sqrt{A(\theta)^2 - B(\theta)^2}}\mathrm{ch}\,(\psi) + \frac{B(\theta)}{\sqrt{A(\theta)^2 - B(\theta)^2}}\mathrm{sh}\,(\psi) = \frac{C(\theta)}{\sqrt{A(\theta)^2 - B(\theta)^2}}. \tag{3.5}$$

Since

$$\frac{A(\theta)}{\sqrt{A(\theta)^2 - B(\theta)^2}} \geq 1,$$

hence there exists δ such that

$$\mathrm{ch}\,(\delta) = \frac{A(\theta)}{\sqrt{A(\theta)^2 - B(\theta)^2}}$$

and

$$\mathrm{sh}\,(\delta) = \frac{B(\theta)}{\sqrt{A(\theta)^2 - B(\theta)^2}}.$$

Then clearly

$$\mathrm{th}\,(\delta) = \frac{B(\theta)}{A(\theta)}.$$

We infer from (3.5) that

$$\mathrm{ch}(\delta + \psi) = \mathrm{ch}\,(\delta)\,\mathrm{ch}\,(\psi) + \mathrm{sh}\,(\delta)\,\mathrm{sh}\,(\psi) = \frac{C(\theta)}{\sqrt{A(\theta)^2 - B(\theta)^2}}.$$

The result follows.

Remark 3.2. A graph of ψ as a function of θ is called the (kinematic) *transmission function*. The transmission function has a very characteristic shape, hence the type of the Minkowskian four-bar linkage can immediately be read from it.

Remark 3.3. Notice that there are two angles ψ for each angle θ. This arises because the moving pivot B of the output crank can be assembled above or below the diagonal joining the moving pivot A of the input crank to the fixed pivot of C.

3.2. **Branching points.** The transmission function gives for any θ two, one, no or an infinite number of values of ψ. No values for ψ exist iff the position of the linkage is impossible. In an 'undetermined position' θ and ψ are independent of each other: at a single θ, an infinite amount of values of ψ is possible or vice versa. We call these θ angles to the *branching points* of the mechanism.

Corollary 3.1. *(Branching points) Suppose that $g \neq b$. Then the branching points of the Minkowskian planar 4R occours at*

$$\theta = arch\left(\frac{a^2 - h^2}{2a(g-b)} + \frac{g-b}{2a}\right). \tag{3.6}$$

Proof. It is clear from Theorem 3.1 that θ is a branching point of the mechanism iff

$$A(\theta) + C(\theta) = 0.$$

This means that

$$2gb - 2ab\mathrm{ch}\,(\theta) + h^2 - g^2 - b^2 - a^2 + 2ag\mathrm{ch}\,(\theta) = 0,$$

that is

$$\mathrm{ch}\,(\theta) = \frac{a^2 - h^2}{2a(g-b)} + \frac{g-b}{2a}.$$

□

Corollary 3.2. *Suppose that $g = b$ and $h \neq a$. Then there is no branching points.*

Proof. If $g = b$ and $h \neq a$, then

$$A(\theta) + C(\theta) = h^2 - a^2 \neq 0.$$

for each θ. □

Corollary 3.3. *Suppose that $g = b$ and $h = a$. Then all points are branching points.*

Proof. This is clear, since then

$$A(\theta) + C(\theta) = 0$$

for each θ. □

Remark 3.4. The deeper investigation of branching points will be one of the topics of our next article.

3.3. **Coupler Angles.** Let ϕ denote the angle between the vectors $\overrightarrow{AO}$ and $\overrightarrow{AB}$ (see Figure 3).

Theorem 3.2. *If ϕ denotes the coupler angle, then*

$$\phi = artanh\left(\frac{bsh\,(\psi) - ash\,(\theta)}{g + bch\,(\psi) - ach\,(\theta)}\right) - \theta$$

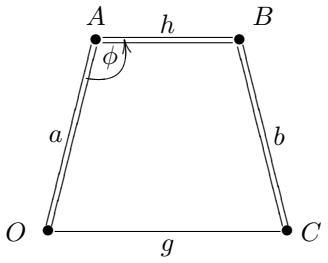

FIGURE 3. The coupler angle

Proof. Since ϕ was the coupler angle, hence $\theta+\phi$ is the angle to AB from the x-axis of F. Consequently we can write the coordinates of B in terms of ϕ as

$$B = (a\mathrm{ch}(\theta) + h\mathrm{ch}(\theta+\phi), a\mathrm{sh}(\theta) + h\mathrm{sh}(\theta+\phi)). \tag{3.7}$$

If we equate the two forms (3.3) and (3.7) for B, we obtain the following loop equations of the four-bar linkage:

$$a\mathrm{ch}(\theta) + h\mathrm{ch}(\theta+\phi) = g + b\mathrm{ch}(\psi)$$
$$a\mathrm{sh}(\theta) + h\mathrm{sh}(\theta+\phi) = b\mathrm{sh}(\psi)$$

Therefore, for a given value of the driving crank θ, $\mathrm{ch}(\theta+\phi)$ and $\mathrm{sh}(\theta+\phi)$ are given by

$$\mathrm{ch}(\theta+\phi) = \frac{g + b\mathrm{ch}(\psi) - a\mathrm{ch}(\theta)}{h}$$

and

$$\mathrm{sh}(\theta+\phi) = \frac{b\mathrm{sh}(\psi) - a\mathrm{sh}(\theta)}{h}.$$

Hence

$$\mathrm{th}(\theta+\phi) = \frac{b\mathrm{sh}(\psi) - a\mathrm{sh}(\theta)}{g + b\mathrm{ch}(\psi) - a\mathrm{ch}(\theta)}$$

and Theorem 3.2 follows. □

Remark 3.5. Notice that we obtain a unique value for ϕ associated with each of the two solutions for the output angle ψ.

3.4. **The transmission angle.** Let ζ denote the angle between the coupler and the driven crank at B, the *transmission angle* of the linkage (see Figure 4).

Theorem 3.3. *If ζ is the transmission angle of the linkage, then*

$$\zeta = arch\left(\frac{-g^2 - a^2 + h^2 + b^2 + 2agch(\theta)}{2bh}\right).$$

Proof. Let $d := \| \overrightarrow{AC} \|$.

To determine ζ in terms of θ, equate the Minkowskian cosine laws (Theorem 2.1) for the diagonal AC for the triangles $\triangle COA$ and $\triangle ABC$. Since ζ is the interior angle at B, we have

$$d^2 = g^2 + a^2 - 2ag\mathrm{ch}(\theta) = h^2 + b^2 - 2bh\mathrm{ch}(\zeta).$$

The result follows □

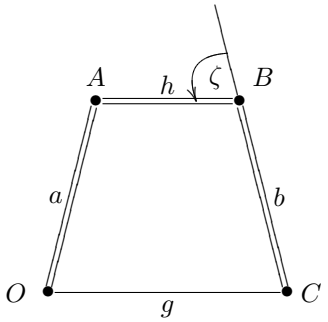

FIGURE 4. The transmission angle

3.5. **The coupler curve.** In this subsection, we study the motion of the coupler by analyzing the curve traced by a point on the coupler link. We get the parametrized equation of this curve, the *coupler curve* from the kinematics equations of the driving RR chain (see Figure 5).

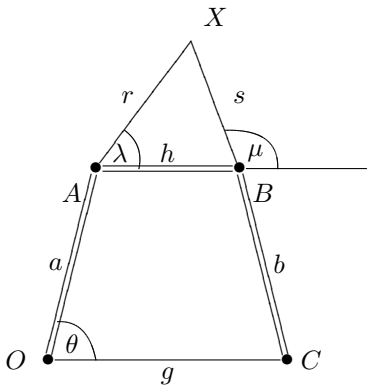

FIGURE 5. The coupler curve

Theorem 3.4. *The curve traced by any point of the coupler link of a Minkowskian planar four-bar linkage is algebraic, of sixth degree.*

Proof. Let $\underline{x} = (x, y)^T$ be the coordinates of a coupler point in the frame M located at A with its x-axis along AB.

Let $\underline{X} = (X, Y)^T$ be the coordinates of a coupler point in the frame F.

We obtain the algebraic equation of the coupler curve by defining the coordinates of $\underline{X} = (X, Y)^T$ from two points of view. Let the coupler triangle $\triangle XAB$ have length r and s given by

$$r = \| \overrightarrow{AX} \| = \sqrt{x^2 - y^2}$$

and

$$s = \| \overrightarrow{BX} \| = \sqrt{(x-h)^2 - y^2}.$$

If λ is the angle to AX in F and μ is the angle to BX (see Figure 5), then we have by definition that

$$\overrightarrow{AX} = (r\mathrm{ch}\,(\lambda)\,, r\mathrm{sh}\,(\lambda))$$

and

$$\overrightarrow{BX} = (s\mathrm{ch}\,(\mu)\,, s\mathrm{sh}\,(\mu)).$$

If we substitute into the identities $\| \overrightarrow{OA} \|^2 = a^2$ and $\| \overrightarrow{CB} \|^2 = b^2$ and rearrange these equations, we obtain

$$(X - s\mathrm{ch}\,(\mu) - g)^2 - (Y - s\mathrm{sh}\,(\mu))^2 = h^2 \tag{3.8}$$

and

$$(X - r\mathrm{ch}\,(\lambda))^2 - (Y - r\mathrm{sh}\,(\lambda))^2 = a^2. \tag{3.9}$$

If we expand equations (3.8) and (3.9), we get

$$2Xs\mathrm{ch}\,(\mu) - 2Ys\mathrm{sh}\,(\mu) - 2gs\mathrm{ch}\,(\mu) - X^2 + 2Xg + Y^2 - g^2 + h^2 - s^2 = 0 \tag{3.10}$$

and

$$2Xr\mathrm{ch}\,(\lambda) - 2Yr\mathrm{sh}\,(\lambda) - X^2 + Y^2 + a^2 - r^2 = 0. \tag{3.11}$$

Let $\gamma := \mu - \lambda$ and substitute $\mu = \lambda + \gamma$ into the equation (3.10).

If we rearrange these equations we get

$$A_1(X,Y)\mathrm{ch}\,(\lambda) + B_1(X,Y)\mathrm{sh}\,(\lambda) = C_1(X,Y),$$

$$A_2(X,Y)\mathrm{ch}\,(\lambda) + B_2(X,Y)\mathrm{sh}\,(\lambda) = C_2(X,Y), \tag{3.12}$$

where

$$A_1(X,Y) := 2Xs\mathrm{sh}\,(\gamma) - 2Ys\mathrm{ch}\,(\gamma) - 2gs\mathrm{sh}\,(\gamma)\,,$$

$$B_1(X,Y) := 2Xs\mathrm{ch}\,(\gamma) - 2Ys\mathrm{sh}\,(\gamma) - 2gs\mathrm{ch}\,(\gamma)\,,$$

$$C_1(X,Y) := X^2 - 2Xg - Y^2 + g^2 - h^2 + s^2,$$

$$A_2(X,Y) := 2rX,$$

$$B_2(X,Y) := -2rY,$$

and

$$C_2(X,Y) := X^2 - Y^2 - a^2 + r^2.$$

We can eliminate λ from the equation system (3.12) by solving linearly for $u = \mathrm{ch}\,(\lambda)$ and $v = \mathrm{sh}\,(\lambda)$. Then we can impose the condition $u^2 - v^2 = 1$. This yields to

$$(C_1(X,Y)B_2(X,Y) - C_2(X,Y)B_1(X,Y))^2 - (A_2(X,Y)C_1(X,Y) - A_1(X,Y)C_2(X,Y))^2 -$$

$$-(A_1(X,Y)B_2(X,Y) - A_2(X,Y)B_1(X,Y))^2 = 0.$$

Notice that $A_i(X,Y)$ and $B_i(X,Y)$ are linear in the coordinates X and Y, and $C_i(X,Y)$ are quadratic. Therefore the equation defines a curve of degree 6. □

3.6. **The input and the output Crank Angles and the classification of the 4R linkage.** The following Theorem describes the upper and the lower limiting angles.

Theorem 3.5. *The upper and the lower limiting angles θ_{max} and θ_{min} that define the range of movement of the input crank,*

$$ch(\theta_{min}) = \frac{a^2 + g^2 - (b+h)^2}{2ag}$$

and

$$ch(\theta_{max}) = \frac{a^2 + g^2 - (b-h)^2}{2ag}.$$

Proof. The formula (see equation (3.1) in Theorem 3.1) that defines the output angle ψ for a given input angle θ has a real solution if and only if $B(\theta)^2 + C(\theta)^2 - A(\theta)^2 \geq 0$. We obtain the maximum and the minimum values for θ if we set this condition to zero, which yields the following quadratic equation in $\mathrm{ch}\,(\theta)$

$$4a^2g^2\mathrm{ch}^2(\theta) - 4ag(g^2 + a^2 - h^2 - b^2)\mathrm{ch}\,(\theta) +$$
$$+((g^2 + a^2) - (h+b)^2)((g^2 + a^2) - (h-b)^2) = 0.$$

The roots of this equation are the given equations for $\mathrm{ch}(\theta_{min})$ and $\mathrm{ch}(\theta_{max})$. □

Remark 3.6. These equations are the cosine laws for the two ways that the triangle $AOC\triangle$ can be formed with the coupler AB aligned with the output crank CB, see Figure 6, Figure 7 and Figure 8.

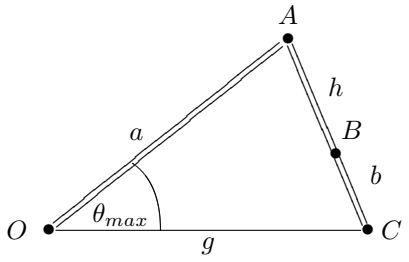

FIGURE 6. The angles θ_{min} and θ_{max} are the limits to the range of movement of the input link

The hyperbolic cosine function does not distinguish between $\pm\theta$, so there are actually two limits for $\mathrm{ch}(\theta_{max})$ above and below OC.

If θ_{max} does not exist, then the crank has no lower limit to its movement and it rotated though $\theta = 0$ to reach negative values below the segment OC.

Thus $\mathrm{ch}(\theta_{max}) < 1$ is the condition that there is no lower limit to the input crank rotation, that is,

$$\frac{a^2 + g^2 - (b-h)^2}{2ag} < 1.$$

We can simplify this to yield

$$(b-h)^2 - (a-g)^2 > 0,$$

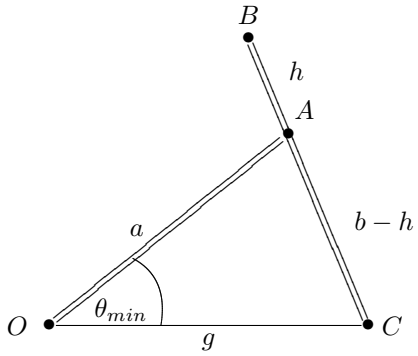

FIGURE 7. The angles θ_{min} and θ_{max} are the limits to the range of movement of the input link

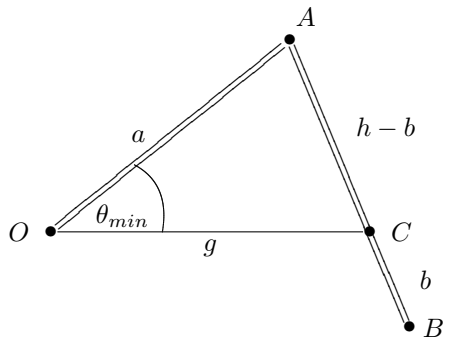

FIGURE 8. The angles θ_{min} and θ_{max} are the limits to the range of movement of the input link

If we factor the difference to two squares, we obtain

$$(-a+g+b-h)(a-g+b-h)>0,$$

that is

$$T_1T_2>0,$$

where $T_1 := -a+g+b-h$ and $T_2 := a-g+b-h$.

If $\mathrm{ch}(\theta_{min})>1$, then both upper and lower limiting angles exist. The input crank rocks in one of three separate ranges: (i) $\theta_{max} \leq \theta \leq \infty$, (ii) $-\theta_{min} \leq \theta \leq \theta_{min}$ or (iii) $-\infty \leq \theta \leq -\theta_{max}$.

It is easy to see that the $\mathrm{ch}(\theta_{min})>1$ condition is equivalent with

$$(g-a-b-h)(g-a+b+h)>0,$$

that is, $T_3T_4>0$, where $T_3 := g-a-b-h$ and $T_4 := g-a+b+h$.

Finally we get the following result:

Theorem 3.6. *We can identify three types of movement available to the input crank of a 4R linkage:*

1. A **crank***: $T_1T_2 \geq 0$ and $T_3T_4 \leq 0$, in which case no θ_{min}, θ_{max} exists, and the input crank rocks though $\theta = 0$.*

2. A **rocker***: $T_1T_2 < 0$ and $T_3T_4 \leq 0$, which means that both upper and lower limiting angles exist, and the crank cannot pass though* 0*. Instead, it rocks in one of the two separate ranges: (i) $\theta_{max} \leq \theta \leq \infty$ or (ii) $-\infty \leq \theta \leq -\theta_{max}$.*

3. A **superrocker***: $T_1T_2 < 0$ and $T_3T_4 > 0$, which means that both upper and lower limiting angles exist. It rocks in one of the three separate ranges: (i) $\theta_{max} \leq$ theta $\leq \infty$, (ii) $-\theta_{min} \leq \theta \leq \theta_{min}$ or (iii) $-\infty \leq \theta \leq -\theta_{max}$.*

□

The range of movement of the output crank can be analyzed in the same way. The limiting positions occur when the input crank OA and the coupler AB become aligned.

Theorem 3.7. *The limits ψ_{max} and ψ_{min} are defined by the equations*

$$ch(\psi_{max}) = \frac{(a+h)^2 - g^2 - b^2}{2bg}$$

and

$$ch(\psi_{min}) = \frac{(a-h)^2 - g^2 - b^2}{2bg}.$$

□

Remark 3.7. In this case ψ is the exterior angle and changes the sign of the hyperbolic cosine term in the cosine law formula.

We find the condition for no lower limit ψ_{max} is

$$\text{ch}(\psi_{max}) = \frac{(a+h)^2 - g^2 - b^2}{2bg} < 1.$$

Hence

$$(a+h)^2 < (b+g)^2$$

that is

$$(g+b+a+h)(g+b-h-a) > 0.$$

Using the notations

$$T_1 := g+b-h-a \text{ and } T_7 := g+b+a+h,$$

we get

$$T_1T_7 > 0.$$

But clearly $T_7 > 0$.

It is easy to see that the condition $\text{ch}(\psi_{min}) > 1$ is equivalent with $(a-h-g-b)(a-h+g+b) > 0$, that is $T_4T_5 < 0$, where $T_4 := -a+h+g+b$ and $T_5 := a-h+g+b$.

Finally we get the following result.

Theorem 3.8. *We can identify three types of movement available to the output crank of a 4R Minkowskian linkage:*

1. A **crank***: $T_1 \geq 0$ and $T_4T_5 \geq 0$, in which case no ψ_{min}, ψ_{max} exists, and the output crank rocks though $\psi = 0$.*

2. A **rocker***: $T_1 < 0$ and $T_4T_5 \geq 0$, which means that both upper and lower limiting angles exist, and the crank cannot pass though* 0*. Instead, it rocks in one of the two separate ranges: (i) $\psi_{max} \leq \psi \leq \infty$ or (ii) $-\infty \leq \psi \leq -\psi_{max}$.*

3. A **superrocker***: $T_1 < 0$ and $T_4T_5 < 0$, which means that both upper and lower limiting angles exist. It rocks in one of the three separate ranges: (i) $\psi_{max} \leq \psi \leq \infty$, (ii) $-\psi_{min} \leq \psi \leq \psi_{min}$ or (iii) $-\infty \leq \psi \leq -\psi_{max}$.*

□

Hence we can classify a Minkowskian planar 4R linkage by the movement of input and output cranks. For example, a crank-rocker has a rotatable input link though O and an output link that rocks.

Now we define special subclasses of the Minkowskian planar 4R mechanisms.

We say that a planar 4R is *normal*, if all the conditions $a+b+h \leq g$, $a+b+g \leq h$, $a+g+h \leq b$ and $b+g+h \leq a$ are satisfied. We say that a planar 4R is *strange* if it is not normal. This means that there exists one link, which is longer than the sum of other links' lengths.

We say that a normal planar 4R is *rigid*, if one of the following conditions is satisfied: $a+b+h = g$, $a+b+g = h$, $a+g+h = b$ and $b+g+h = a$.

We say that a nonrigid normal planar 4R is *irreducible*, if $T_1 \neq 0$ and $T_2 \neq 0$, i.e., $a+h \neq b+g$ and $a+b \neq g+h$.

Finally we say that a nonrigid normal planar 4R, which is not irreducible, is a *reducible* planar 4R.

First we investigate the strange mechanisms.

Theorem 3.9. *Suppose that $g > a+b+h$. Then the Minkowskian planar 4R has a superrocker–crank type.*

Proof. Since $T_1 > 0$, $T_2 < 0$, $T_3 > 0$, $T_4 > 0$ and $T_5 > 0$.

□

Theorem 3.10. *Suppose that $a > g+b+h$. Then the Minkowskian planar 4R has a superrocker–superrocker type.*

Proof. Since $T_1 < 0$, $T_2 > 0$, $T_3 < 0$, $T_4 < 0$ and $T_5 > 0$.

□

Theorem 3.11. *Suppose that $h > g+b+a$. Then the Minkowskian planar 4R has a crank–superrocker type.*

Proof. Since $T_1 < 0$, $T_2 < 0$, $T_3 < 0$, $T_4 > 0$ and $T_5 < 0$.

□

Theorem 3.12. *Suppose that $b > g+h+a$. Then the Minkowskian planar 4R has a crank–crank type.*

Proof. Since $T_1 > 0$, $T_2 > 0$, $T_3 < 0$, $T_4 > 0$ and $T_5 > 0$. □

We summarized the classification of strange mechanisms in Table 1.

In the following we consider only normal mechanisms.

Here we investigate first the rigid mechanisms.

Theorem 3.13. *Suppose that $g = a+b+h$. Then the Minkowskian planar 4R has a rocker–crank type.*

Proof. Since $T_1 > 0$, $T_2 < 0$, $T_3 = 0$, $T_4 > 0$ and $T_5 > 0$.

□

Theorem 3.14. *Suppose that $a = g+b+h$. Then the Minkowskian planar 4R has a rocker–rocker type.*

	Linkage Type	Condition
1	Crank–Crank	$b > g + h + a$
2	Crank–Superrocker	$h > g + b + a$
3	Superrocker–crank	$g > a + b + h$
4	Superrocker–superrocker	$a > g + b + h$

TABLE 1. Basic Planar 4R *Strange* Linkage Types

Proof. Since $T_1 < 0$, $T_2 > 0$, $T_3 < 0$, $T_4 = 0$ and $T_5 > 0$. □

Theorem 3.15. *Suppose that $h = g + b + a$. Then the Minkowskian planar 4R has a crank–rocker type.*

Proof. Since $T_1 < 0$, $T_2 < 0$, $T_3 < 0$, $T_4 > 0$ and $T_5 = 0$. □

Theorem 3.16. *Suppose that $b = g + h + a$. Then the Minkowskian planar 4R has a crank–crank type.*

Proof. Since $T_1 > 0$, $T_2 > 0$, $T_3 < 0$, $T_4 > 0$ and $T_5 > 0$. □

We summarized the classification of rigid mechanisms in Table 2.

	Linkage Type	Condition
1	Crank–Crank	$b = g + h + a$
2	Crank–Rocker	$h = g + b + a$
3	Rocker–crank	$g = a + b + h$
4	Rocker–Rocker	$a = g + b + h$

TABLE 2. Basic Planar 4R *Rigid* Linkage Types

Now we consider normal, non–rigid reducible linkages.

Theorem 3.17. *Suppose that $g + b = a + h$. Then the Minkowskian planar 4R has a crank–crank type.*

Proof. Since $T_1 = 0$, hence $T_1 T_2 = 0$. □

Theorem 3.18. *Suppose that $a + b = g + h$. Then the input crank is crank.*

Proof. Since $T_2 = 0$, hence $T_1 T_2 = 0$. □

Finally we investigate non–rigid normal Minkowskian planar 4R mechanisms.

Theorem 3.19. *For all non–rigid normal Minkowskian planar 4R we have $T_3 < 0$, $T_4 > 0$ and $T_5 > 0$.*

The link lengths a, b, g and h for a 4R chain define the two parameters T_1, T_2. Clearly our classification requires only the signs of these parameters. We assamble here an array for $(\mathrm{sgn}T_1, \mathrm{sgn}T_2)$ (see Table 3).

	Linkage Type	T_1	T_2
1	Crank–crank	+	+
2	Rocker–crank	+	−
3	Rocker–rocker	−	+
4	Crank–rocker	−	−

TABLE 3. Basic Planar 4R *Normal Non–Rigid* Linkage Types

Remark 3.8. It is easy to see from the reversed triangle inequality (Lemma 2.2) that the following criterion is analogous to Grashof's criterion:

$$l + s \geq p + q,$$

where s is the length of the shortest link, l is the length of the longest link and p, q are the lengths of the remaining two links.

3.7. **Examples.** We animated the movement of the Minkowskian planar 4R in Matlab. In the following examples we show some pictures from our animation.

1. Suppose that $a := 1$, $b := 1$, $g := 4$ and $h := 1$. Then $g > a + b + h$, hence this is a *strange* Minkowskian planar 4R. We get

$$\begin{aligned} \mathrm{ch}(\theta_{min}) &= 1.625, \\ \mathrm{ch}(\theta_{max}) &= 2.125, \\ \mathrm{ch}(\psi_{min}) &= -2.125, \\ \mathrm{ch}(\psi_{max}) &= -1.625. \end{aligned}$$

$T_1 = g + b - h - a = 3$, $T_2 = a - g + b - h = -3$, $T_3 = g - a - b - h = 1$, $T_4 = g - a + b + h = 5$ and $T_5 = a - h + g + b = 5$. Since $T_1 > 0$, $T_2 < 0$, $T_3 > 0$, $T_4 > 0$ and $T_5 > 0$, thus this planar 4R has a superrocker–crank type.

The branching points occour at $\mathrm{ch}\,(\theta) = 1.5$.

We show here two pictures from the animation (see Figures 9, 10), the coupler curve (Figure 11) and the transmission curve (Figure 12). In Figure 11 the blue (resp. dashed) curve shows the trajectory of the end of the input crank, the black (resp. thick) curve shows the trajectory of the middle point of the coupler, while the red (resp. solid) curve shows the trajectory of the end of the input crank

2. Suppose that $a := 1.2$, $b := 0.4$, $g := 0.4$ and $h := 0.4$. Then $a = g + b + h$, hence this is a rigid Minkowskian planar 4R. We get

$$\begin{aligned} \mathrm{ch}(\theta_{min}) &= 1, \\ \mathrm{ch}(\theta_{max}) &\approx 1.6666, \\ \mathrm{ch}(\psi_{min}) &= 1, \\ \mathrm{ch}(\psi_{max}) &= 7. \end{aligned}$$

$T_1 = g + b - h - a = -0.8$, $T_2 = a - g + b - h = 0.8$, $T_3 = g - a - b - h = -1.6$, $T_4 = g - a + b + h = 0$ and $T_5 = a - h + g + b = 1.6$. Since $T_1 < 0$, $T_2 > 0$, $T_3 < 0$, $T_4 = 0$ and $T_5 > 0$, thus this planar 4R has a rocker–rocker type.

Here $g = b$, but $h \neq a$, hence there are no branching points.

We show here two pictures from the animation (Figures 13, 14), the coupler curve (Figure 15) and the transmission curve (Figure 16). In Figure 15 the blue (resp. dashed) curve shows the trajectory of the end of the input crank, the black

(resp. thick) curve shows the trajectory of the middle point of the coupler, while the red (resp. solid) curve shows the trajectory of the end of the input crank

3. Suppose that $a := 0.5$, $b := 1$, $g := 2$ and $h := 2.5$. Then $g + b = a + h$, hence this is a normal, non–rigid reducible Minkowskian planar 4R. We get

$$\mathrm{ch}(\theta_{min}) = -4,$$

$$\mathrm{ch}(\theta_{max}) = 1,$$

$$\mathrm{ch}(\psi_{min}) = -0.25,$$

$$\mathrm{ch}(\psi_{max}) = 1.$$

Hence $T_1 = g + b - h - a = 0$, $T_2 = a - g + b - h = -3$, $T_3 = g - a - b - h = -2$, $T_4 = g - a + b + h = 5$ and $T_5 = a - h + g + b = 1$. Since $T_1 = 0$, $T_2 < 0$, $T_3 < 0$, $T_4 > 0$ and $T_5 > 0$, thus this planar 4R has a crank–crank type.

The branching points occour at $\mathrm{ch}(\theta) = -5$, hence there are no branching points..

We show here two pictures from the animation (Figures 17, 18), the coupler curve (Figure 19) and the transmission curve (Figure 20). In Figure 19 the blue (resp. dashed) curve shows the trajectory of the end of the input crank, the black (resp. thick) curve shows the trajectory of the middle point of the coupler, while the red (resp. solid) curve shows the trajectory of the end of the input crank

4. Suppose that $a := 0.6$, $b := 1$, $g := 0.7$ and $h := 0.5$. Then this is a normal, non–rigid irreducible Minkowskian planar 4R. We get

$$\mathrm{ch}(\theta_{min}) \approx -1.6666,$$

$$\mathrm{ch}(\theta_{max}) \approx 0.71428,$$

$$\mathrm{ch}(\psi_{min}) \approx -1.05714,$$

$$\mathrm{ch}(\psi_{max}) = -0.2.$$

Hence $T_1 = g + b - h - a = 0.6$, $T_2 = a - g + b - h = 0.4$, $T_3 = g - a - b - h = -1.4$, $T_4 = g - a + b + h = 1.6$ and $T_5 = a - h + g + b = 1.8$. Since $T_1 > 0$, $T_2 > 0$, $T_3 < 0$, $T_4 > 0$ and $T_5 > 0$, thus this planar 4R has a crank–crank type.

The branching points occour at $\mathrm{ch}(\theta) \approx -0.5555$, hence there are no branching points..

We show here two pictures from the animation (Figures 21,22), the coupler curve (Figure 23) and the transmission curve (Figure 24). In Figure 23 the blue (resp. dashed) curve shows the trajectory of the end of the input crank, the black (resp. thick) curve shows the trajectory of the middle point of the coupler, while the red (resp. solid) curve shows the trajectory of the end of the input crank

4. Conclusion

In this article we characterized and classified completely the planar 4R closed chain working on the Minkowskian plane. We derived formulas for the output crank angle, the coupler angle and the transmission angle. We found four basic types in the classification: the crank-crank, crank–rocker, rocker–crank and rocker–rocker Minkowskian planar 4R mechanisms and we described the Minkowskian Grashof condition.

Acknowledgements. The authors are grateful to Josef Schicho, Hans–Peter Schröcker and Madalina Hodorog for their useful comments.

References

[1] Birman, G. S. and Nomizu, K., Trigonometry in Lorentzian geometry. *Amer. Math. Monthly* **91** (1984), no. 9, 543–549.

[2] Catoni, F., Cannata R., Catoni, V. and Zampetti, P., Hyperbolic trigonometry in two-dimensional space-time geometry. *Nuovo Cimento Soc. Ital. Fis.* B **118** (2003), no. 5, 475–492.

[3] Catoni, F., Cannata R., Catoni, V. and Zampetti, P., Two-dimensional hypercomplex numbers and related trigonometries and geometries *Adv. Appl. Clifford Algebr.* **14** (2004), no. 1, 47–68.

[4] Ergin, A. A., On the 1-parameter Lorentzian motions, Comm. Fac. Sci. Univ. Ankara Ser. A_1 Math. Statist. 40 (1991), 59–66.

[5] Einstein, A., Zur Elektrodynamik bewegter Körper, *Annalen der Physik* **322**, (1905) Issue 10, 895–921.

[6] Fjelstad, P. and Gal, S. G., Two-dimensional geometries, topologies, trigonometries and physics generated by complex-type numbers. *Adv. Appl. Clifford Algebras* **11** (2001), no. 1, 81–107

[7] Gündoğan, H. and Keçilioğlu, O., Lorentzian matrix multiplication and the motions on Lorentzian plane. *Glas. Mat. Ser.* III **41(61)** (2006), no. 2, 329–334.

[8] Harkin, A. A. and Harkin, J. B., Geometry of Generalized Complex Numbers. *Math. Mag.* **77** (2004), no. 2, 118–129.

[9] Lie, S. and Scheffers, M. G., Vorlesungen über continuierliche Gruppen, Kap. 21, Teubner, Leipzig, 1893

[10] McCarthy, J. M., Geometric design of linkages. Interdisciplinary Applied Mathematics, **11** Springer-Verlag, New York, 2000.

[11] McCarthy, J. M., An Introduction to Theoretical Kinematics, MIT Press, Cambridge, 1990.

[12] Myrvold, W.C. and Christian, J., Quantum Reality, Relativistic Causality and closing the epistemic circle, Springer Science+Business Media, 2009.

[13] O'Neill, B., Semi-Riemannian Geometry. With Applications to Relativity, Academic Press, Inc., New York, 1983.

[14] Nešović, E. and Petrović-Torgašev, M., Some trigonometric relations in the Lorentzian plane. Kragujevac J. Math. **25** (2003), 219–225.

[15] Ratcliffe, J. G., Foundations of Hyperbolic Manifolds, Springer-Verlag, New York, 1994.

[16] Yaglom, I. M., A simple non-Euclidean geometry and its physical basis. An elementary account of Galilean geometry and the Galilean principle of relativity. Springer-Verlag, New York-Heidelberg, 1979

[17] Yüce, S. and Kuruğlu, N., One-parameter plane hyperbolic motions. *Adv. Appl. Clifford Algebr.* **18** (2008), no. 2, 279–285.

Kecskemet College, Kecskemet, Hungary
E-mail address: gabor.hegedues@oeaw.ac.at

Advanced Telecommunications Research Institute International, Cognitive Mechanisms Laboratory, Kyoto, Japan

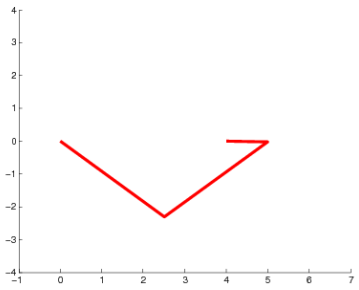

FIGURE 9. The Minkowskian planar 4R with $a = 1$, $b = 1$, $h = 1$, $g = 4$ at $\theta = -\pi/2$

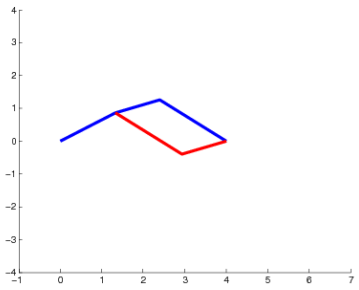

FIGURE 10. The Minkowskian planar 4R with $a = 1$, $b = 1$, $h = 1$, $g = 4$ at $\theta = \pi/4$

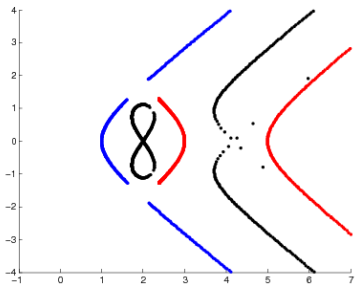

FIGURE 11. The coupler curve of the Minkowskian planar 4R with $a = 1$, $b = 1$, $h = 1$, $g = 4$

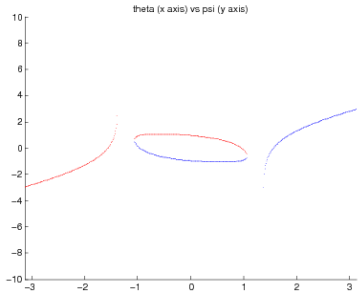

FIGURE 12. The transmission function of the Minkowskian planar 4R with $a = 1$, $b = 1$, $h = 1$, $g = 4$

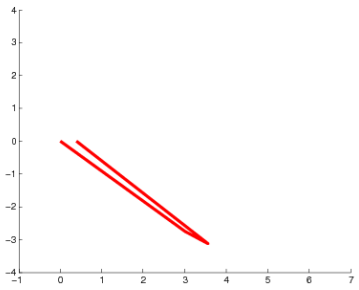

FIGURE 13. The Minkowskian planar 4R with $a = 1.2$, $b = 0.4$, $h = 0.4$, $g = 0.4$ at $\theta = -\pi/2$

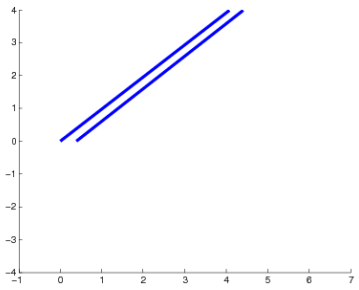

FIGURE 14. The Minkowskian planar 4R with $a = 1.2$, $b = 0.4$, $h = 0.4$, $g = 0.4$ at $\theta = 3\pi/4$

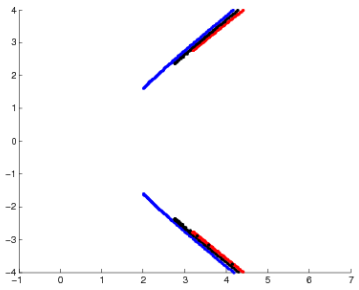

FIGURE 15. The coupler curve of the Minkowskian planar 4R with $a = 1.2$, $b = 0.4$, $h = 0.4$, $g = 0.4$

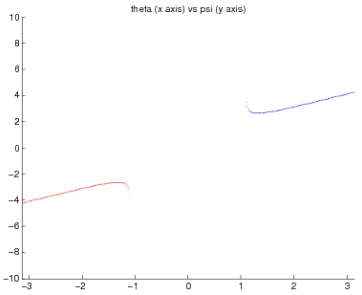

FIGURE 16. The transmission function of the Minkowskian planar 4R with $a = 1.2$, $b = 0.4$, $h = 0.4$, $g = 0.4$

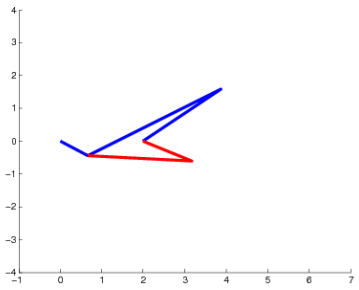

FIGURE 17. The Minkowskian planar 4R with $a := 0.5$, $b := 1$, $g := 2$, $h := 2.5$ at $\theta = -\pi/4$

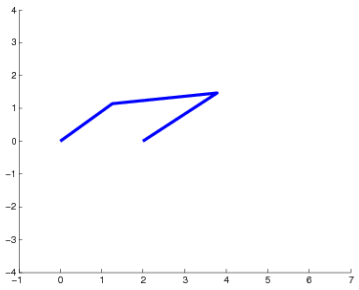

FIGURE 18. The Minkowskian planar 4R with $a := 0.5$, $b := 1$, $g := 2$, $h := 2.5$ at $\theta = \pi/2$

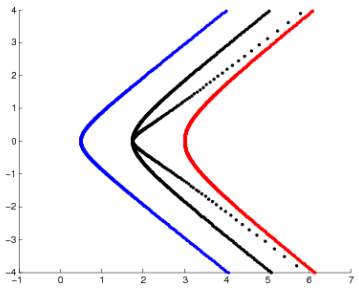

FIGURE 19. The coupler curve of the Minkowskian planar 4R with $a := 0.5$, $b := 1$, $g := 2$, $h := 2.5$

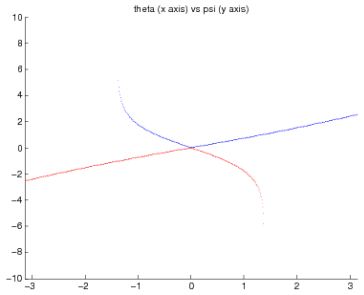

FIGURE 20. The transmission function of the Minkowskian planar 4R with $a := 0.5$, $b := 1$, $g := 2$, $h := 2.5$

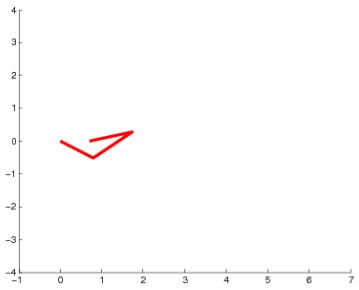

FIGURE 21. The Minkowskian planar 4R with $a := 0.6$, $b := 1$, $g := 0.7$, $h := 0.5$ at $\theta = -\pi/4$

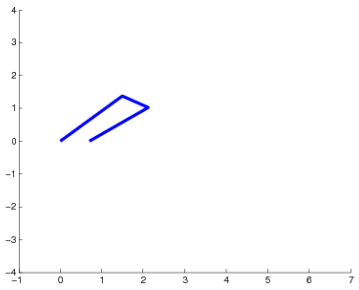

FIGURE 22. The Minkowskian planar 4R with $a := 0.6$, $b := 1$, $g := 0.7$, $h := 0.5$ at $\theta = \pi/2$

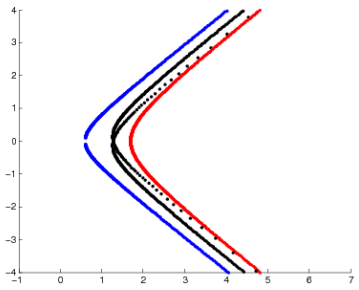

FIGURE 23. The coupler curve of the Minkowskian planar 4R with $a := 0.6$, $b := 1$, $g := 0.7$, $h := 0.5$

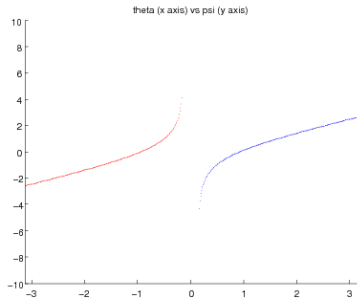

FIGURE 24. The transmission function of the Minkowskian planar 4R with $a := 0.6$, $b := 1$, $g := 0.7$, $h := 0.5$